

PAPER • OPEN ACCESS

## Phase transformations in Ni-Ti SMA spring

To cite this article: K. K. Mahesh and F. M. Braz Fernandes 2023 *J. Phys.: Conf. Ser.* **2603** 012017

View the [article online](#) for updates and enhancements.

You may also like

- [On the impact of lattice parameter accuracy of atomistic simulations on the microstructure of Ni-Ti shape memory alloys](#)  
L La Rosa and F Maresca
- [Microstructure, hardness and corrosion behavior of Ni-Ti alloy with the addition of rare earth metal oxide \(Gd<sub>2</sub>O<sub>3</sub>\)](#)  
Yang Xian Yan, Tahir Ahmad, Xuehui Zhang et al.
- [Investigation of Titanium Supported Nanostructured Au-Ni and Pt-Ni Thin Layers as Electrocatalysts for DBFC](#)  
L. Tamašauskait-Tamašinait, A. Balinait, R. ekaviit et al.

**PRIME**  
PACIFIC RIM MEETING  
ON ELECTROCHEMICAL  
AND SOLID STATE SCIENCE

HONOLULU, HI  
Oct 6–11, 2024

Abstract submission deadline:  
**April 12, 2024**

Learn more and submit!

**Joint Meeting of**  
The Electrochemical Society  
•  
The Electrochemical Society of Japan  
•  
Korea Electrochemical Society

## Phase transformations in Ni-Ti SMA spring

K. K. Mahesh<sup>1\*</sup> and F. M. Braz Fernandes<sup>2</sup>

<sup>1</sup>Department of Physics, Nagarjuna College of Engineering and Technology, Bengaluru, India.

<sup>2</sup>CENIMAT/I3N, Departamento de Ciência dos Materiais, Faculdade de Ciências e Tecnologia, FCT, Universidade Nova de Lisboa, 2829-516 Caparica, Portugal.

\*Corresponding author's e-mail: <kkmahesh@rediffmail.com>

**Abstract.** Equi-atomic Nickel-Titanium (Ni-Ti) alloy is one of the prominent materials to exhibit two way shape memory effect (TWSME). Since the material by itself can change shape due to variation in temperature, it is also used as an actuator. In the present study, Ni-Ti (49.5at%Ni-Ti) alloy wire is converted into a spring coil with straight portions on either ends by shape setting. Training is provided to the spring coil portion to achieve TWSME. Separate specimens from the spring and straight portions were extracted. Phase transformations were observed in the spring and straight portions during heating and cooling. Phase transformation behaviour of the spring coil and straight portions were studied using differential scanning calorimetry (DSC). The straight portion undergoes simple thermal cycles. But the spring coil portion undergoes thermomechanical (TM) cycles due to change in shapes during heating and cooling. The thermograms obtained show difference in their nature of phase transformations. Discussion focusses on the difference in the thermograms appearing for the specimens from straight and coil portions.

### 1. Introduction

Shape memory effect (SME) observed in some of the alloys is attributed to thermoelastic martensite phase transformation. There are several studies found in the literature to understand the phase transformations in these alloys but, most of them separately deal with either thermal or stress induced phase transformations [1, 2]. It is also shown that for a given Ni-Ti alloy system, the phase transformation sequence is influenced by the thermal and mechanical cycling [3-5]. For instance, thermal induced phase transformation temperatures decrease during the early thermal cycles followed by the emergence of stable R-phase transformation [3, 6]. The micromechanics of the transformation temperature drift have yet to be conclusively established, although both the influence of dislocations and the development of martensitic texture have been hypothesized as contributing factors [7]. It is suggested that the development of preferentially oriented R-phase variants in Ni-Ti results in the excellent two way shape memory effect (TWSME) [8].

To observe TWSME, repeated temperature and deformation cycles known as 'training' is required [9, 10]. During the training procedure, both thermal and stress induced phase transformations occur. For thermally-induced martensite all martensitic variants grow by the self-accommodating method in the parent phase matrix, while the stress-induced martensite variant with the orientation preferring to the applied stress [11]. Therefore, in order to understand the mechanism of SME, the alloy should be studied while undergoing TWSME. In the present study, Ni-Ti (49.5at%Ni-Ti) alloy in the wire form is converted into a spring by shape setting. The spring is trained to exhibit TWSME by subjecting it to thermomechanical training (TMT) cycles. Differential Scanning Calorimeter (DSC) thermograms

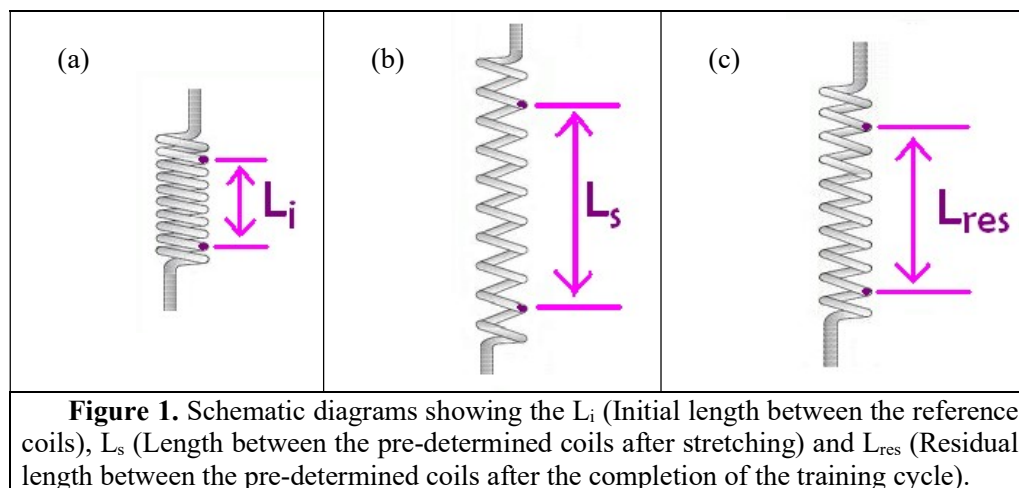


of the thermally cycled versus thermomechanically trained sections during TWSME were obtained. The difference in the nature of phase transformation is presented and discussed to understand the mechanism of TWSME.

## 2. Experimental Procedure

Ni49.5at%-Ti alloy wire of diameter 0.636 mm was obtained from Memory-Metalle GmbH, Germany. The as-received (AR) condition was straight annealed, surface pickled and having active  $A_f = 74$  °C. The wire was converted into a spring by winding it on a mandrel with minor diameter = 4.65 mm and pitch = 0.8 mm. The ends of the wire were kept unwound to remain straight. The spring section was fastened and kept at shape setting temperature of 520 °C for 20 min, and water quenched to room temperature (RT). During this stage of the process, straight section had undergone a simple heat treatment at 520 °C.

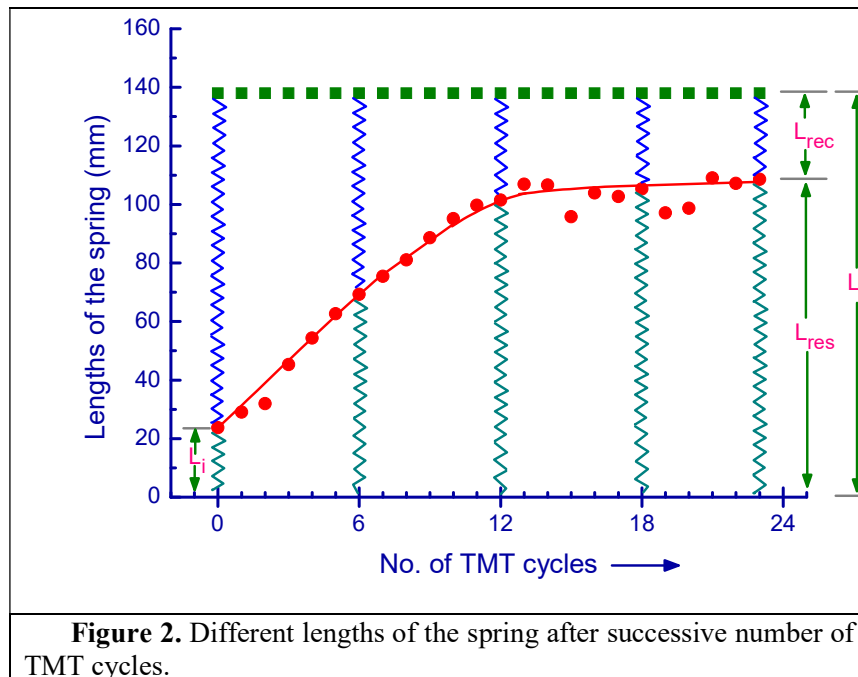
In the spring formed, two different coils were used as reference for the initial length ( $L_i = 24$  mm) as shown in the schematic figure 1a. The spring section was subjected to TMT as follows. At RT, the spring coil was stretched (figure 1b) to a length between the reference coils ( $L_s$ ) equal to 138 mm and placed in the furnace at temperature 150 °C, for 1 min. When the spring was taken out of the furnace, it was water quenched to RT. These steps complete one TMT cycle comprising one-way shape memory effect (OWSME) for the spring section. The straight end section had undergone a simple thermal cycling. At RT, the residual length between the pre-determined coils ( $L_{res}$ ), as shown in figure 1c, was measured to be 29 mm. Training cycle was continued until the spring attained TWSME and the recovery length ( $L_{rec}$ ) gets stabilized.  $L_{res}$  was measured at RT after successive training cycles and the  $L_{rec}$  between the reference coils was calculated as  $L_{rec} = L_s - L_{res}$ . Two pieces of specimens were cut, one from the straight section and the other from the spring section for the DSC analyses, which had undergone simple heat treatment followed by 23 thermal cycles and shape setting followed by 23 TMT cycles, respectively.



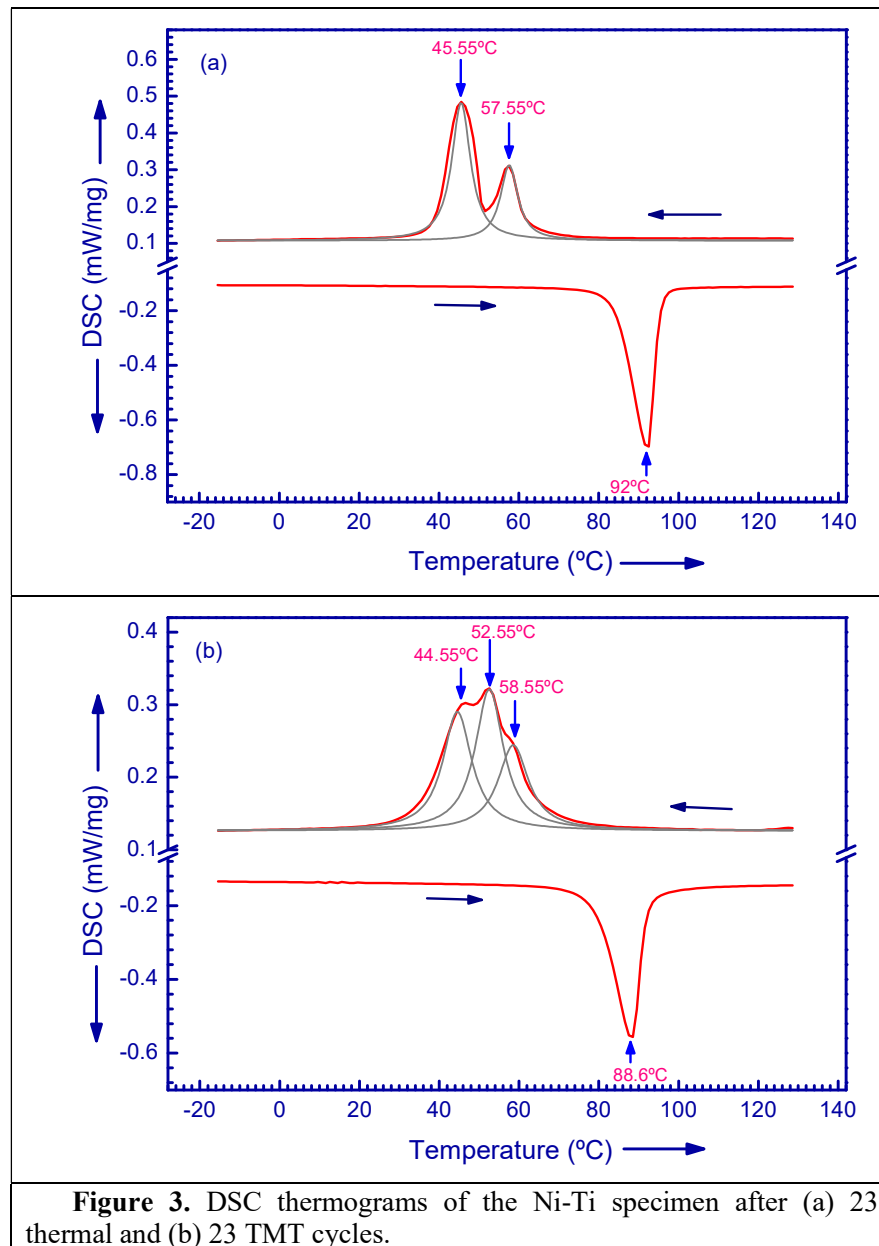
The specimens cut for the DSC analyses were subjected to chemical etching with the solution composition, 10%vol. HF, 45%vol. HNO<sub>3</sub> and 45%vol. H<sub>2</sub>O to get rid of the oxide layer formed during heat treatment and the deformed regions formed during the cutting process. Phase transformations were determined by employing Netzsch DSC 204 F1 Phoenix. Specimen pieces were encapsulated in an aluminum crucible and the DSC measurements were carried out in the temperature range between -50 and 150 °C with a heating and cooling rate of 10K/min. The thermogram peaks were analyzed by using the softwares, Netzsch Proteus – Thermal Analysis supplied with the DSC equipment.

### 3. Results and Discussion

During the TMT process,  $L_{res}$  was measured at RT after successive training cycles and the  $L_{rec}$  between the reference coils were calculated. In figure 2, variation of different lengths ( $L_s$ ,  $L_{res}$  and  $L_{rec}$ ) of the spring with number of TMT cycles is presented.  $L_s$ , the measure of stretched length during the first step of every TMT cycles is kept constant. It can be observed that  $L_{res}$  at RT increases during the initial 14 TMT cycles and, after that, it tends to stabilize to approximately 106 mm. This means that TWSME is established by 14 TMT cycles and on further cycling  $L_{rec}$  remains constant around 32 mm. During TWSME, while heating from RT to 150 °C, the spring contracts from 106 mm to 24 mm, and, after cooling to RT, expands again to 106 mm.



Figures 3a & b shows the DSC thermograms of the wire section which had undergone 23 simple thermal cycles and spring section which, had undergone 23 TMT cycles, respectively. In figure 3a, the DSC thermogram of the straight section with 23 thermal cycles, during the heating part, one endothermic peak representing one-step phase transformation is observed. In the cooling part, two exothermic peaks merged together are observed indicating two-step phase transformation. Figure 3b shows the DSC thermogram of the spring section with 23 TMT cycles. While heating, one-step phase transformation is observed. During cooling, three exothermic peaks merged together are observed. For the straight section with 23 simple thermal cycles, the phase transformations while heating are attributed to martensite (M)  $\rightarrow$  austenite (A) and, while cooling, to austenite (A)  $\rightarrow$  R-phase (R) and R  $\rightarrow$  M. From the DSC thermogram (figure 3a), the phase transformation temperatures obtained are as follows: while heating,  $A_s = 83.6$  °C,  $A_f = 95.7$  °C and while cooling,  $R_s = 63.5$  °C,  $R_f = 53.5$  °C,  $M_s = 52$  °C and  $M_f = 40$  °C. For the spring section with 23 TMT cycles, the phase transformation during heating can be attributed to M  $\rightarrow$  A with  $A_s = 78.9$  °C and  $A_f = 92.9$  °C. However, while cooling, the combination of three exothermic peaks indicates that one more phase transformation process is taking place. The origin of the third peak is discussed below.



In the case of the specimen which had previously undergone 23 simple thermal cycles, during the DSC scanning it was undergoing the 24<sup>th</sup> thermal cycle. It is important to mention here that, this specimen did not undergo shape change during the thermal cycling. The phase transformations taking place during the thermal cycling were thermally-induced. For thermally-induced martensite, all martensitic variants grow by the self-accommodating method in the parent phase matrix [9]. Hence, in the present study, for the specimen extracted from the straight section of the spring that was only subjected to thermal cycles (figure 3a), two exothermic peaks with peak temperatures, 57.55 and 45.55 °C were identified, corresponding to two-step self-accommodating martensite phase transformations, A→R and R→M. But, in the case of the spring coil, 23 TMT cycles involve repeated thermal and deformation cycles. The repeated pattern of deformation during the training cycle could result in the formation of complex dislocation arrays which have the lowest energy in the repeatedly induced ‘trained’ variants [12]. The resulting dislocation structure guides the formation of martensite

variants of preferential orientations, thus resulting in a macroscopic shape change during subsequent thermal transformation cycles [13]. In figure 3b, for the trained spring section, three exothermic peaks while cooling with peak temperatures, 58.55, 52.55 and 44.55 °C could be attributed to A→R phase transformation by self-accommodation, A→M phase transformation by preferential orientation and R→M phase transformation by self-accommodation, respectively. The transformation temperatures obtained after resolving the peaks as shown in figure 3b are  $R_s = 68$  °C,  $R_f = 50$  °C,  $M_{s(PO)} = 62.5$  °C,  $M_{f(PO)} = 42.5$  °C,  $M_s = 53$  °C and  $M_f = 35.5$  °C, where suffix (PO) represents the phase transformation due to preferential orientation. However, while heating, for both the specimens, single endothermic peaks appear with peak temperatures, 92 °C for the specimen with previous simple thermal cycling and 88.6 °C for the specimen with previous TMT. This is in agreement with the finding that there are several ways in which martensite can form from austenite, but there is only one possible route which will return the austenite structure [10, 14].

Shape setting followed by TMT cycling results in the detwinned martensite formation upon cooling. Detwinned martensite formation takes place due to the preferential orientation, rather than self-accommodation, causing spontaneous shape change. It is important to note that during the stress induced martensite transformation, external loading induces a phase transformation from austenite to detwinned martensite. Also, upon loading at low temperatures, the twinned martensite undergoes detwinning/reorientation, resulting in an oriented microstructure with accompanying macroscopic strain [15]. However during TWSME, it is the thermal effect which acts as a driving force to produce internal transformation stress for the subsequent detwinning by preferential orientation.

#### 4. Conclusion

Shape setting was performed for the Ni49.5at%-Ti alloy wire to form a spring. When this spring was subjected to thermomechanical training cycles, following observations are made.

(1) During the initial training cycles, the residual length at RT increases up to the 14th cycle, stabilizing afterwards and exhibiting TWSME.

(2) During the cooling part, for the straight section that was subjected to 23 simple thermal cycling, two-step phase transformation was observed. But, for the spring coil section having undergone 23 thermomechanical training cycles, three different phase transformations were observed. However, during the heating part, for both the sections, single step phase transformation is found to be present.

(3) The extra exothermic peak observed for the specimen that undergone 23 thermomechanical training cycles is attributed to the martensite phase formation due to preferential orientation developed during the training process.

#### Acknowledgements

The authors would like to acknowledge the financial support by Fundação para a Ciência e a Tecnologia – Ministério da Educação e Ciência, Portugal to CENIMAT/I3N through the Strategic Project Ref.: LA 25 – 2011-2012 and Research Project, Smart Composites, Ref.: PTDC/CTM/66380/2006. KKM gratefully acknowledges the fellowship under the scheme, 'Ciência 2007' with Ref.: C2007-443-CENIMAT-6/Ciência2007.

#### References

- [1] Todoroki T and Tamura H, 1987 Effect of Heat Treatment after Cold Working on the Phase Transformation in TiNi Alloy, *T Jpn I Met* **28** 83-94. DOI:10.2320/MATERTRANS1960.28.83
- [2] Brinson L C, Schmidt I and Lammering R, 2004 Stress-induced transformation behavior of a polycrystalline NiTi shape memory alloy: micro and macromechanical investigations via in situ optical microscopy, *J Mech Phys Solids* **52** 1549-1571. DOI: <https://doi.org/10.1016/j.jmps.2004.01.001>

- [3] Pelosin V and Riviere A, 1998 Effect of Thermal Cycling on the R-Phase and Martensitic Transformations in a Ti-Rich NiTi Alloy, *Metall Mater Trans A* **29** 1175-1180. DOI: <https://doi.org/10.1007/s11661-998-0244-5>
- [4] Pattabi M, Ramakrishna K and Mahesh K K, 2007 Effect of thermal cycling on the shape memory transformation behavior of NiTi alloy: Powder X-ray diffraction study, *Mat Sci Eng A-Struct* **448** 33-38. DOI: <https://doi.org/10.1016/j.msea.2006.09.052>
- [5] Paula A S, Mahesh K K and Braz Fernandes F M, 2011 Stability in Phase Transformation After Multiple Steps of Marforming in Ti-Rich Ni-Ti Shape Memory Alloy, *J Mater Eng Perform* **20** 771-775. DOI: <https://doi.org/10.1007/s11665-011-9920-5>
- [6] Soheil Saedi, Ali Sadi Turabi, Mohsen Taheri Andani, Christoph Haberland, Haluk Karaca, Mohammad Elahinia, 2016 The influence of heat treatment on the thermomechanical response of Ni-rich NiTi alloys manufactured by selective laser melting *J. Alloys Compd.*, **677**(25), 204-210. DOI: <https://doi.org/10.1016/j.jallcom.2016.03.161>
- [6] Jones N G, Raghunathan S L and Dye D, 2010 In-Situ Synchrotron Characterization of Transformation Sequences in TiNi-Based Shape Memory Alloys during Thermal Cycling, *Metall Mater Trans A* **41** 912-921. DOI: <https://doi.org/10.1007/s11661-009-0166-x>
- [7] Chang C Y, Vokoun D and Hu C T, 2001 Two-Way Shape Memory Effect of NiTi Alloy Induced by Constraint Aging Treatment at Room Temperature, *Metall Mater Trans A* **32** 1629-1634. DOI: <https://doi.org/10.1007/s11661-001-0141-7>
- [8] Huang X, Ackland G J and Rabe K M, 2003 Crystal structures and shape-memory behaviour of NiTi, *Nat Mater* **2** 307-311. DOI: <https://doi.org/10.1038/nmat884>
- [10] Renhao Liu, Chen Zhang, Hongli Ji, Chao Zhang and Jinhao Qiu, 2023 Training, Control and Application of SMA-Based Actuators with Two-Way Shape Memory Effect, *Actuators* **12**(1), 25. DOI: <https://doi.org/10.3390/act12010025>
- [9] He X M, Rong L J, Yan D S and Li Y Y, 2005 Temperature memory effect of Ni<sub>47</sub>Ti<sub>44</sub>Nb<sub>9</sub> wide hysteresis shape memory alloy, *Scripta Mater* **53** 1411-1415. DOI: <https://doi.org/10.1016/j.scriptamat.2005.08.022>
- [10] van Humbeeck J and Stalmans R, 1999, Characteristics of Shape Memory Alloys, Shape Memory Materials, Ed. Otsuka K and Wayman C M (Cambridge University Press, Cambridge, UK) p.159.
- [11] Wang Z G, Zu X T, Fu P, Dai J Y, Zhu S and Wang L M, 2003 Two-way shape memory effect of TiNi alloy coil extension springs, *Mat Sci Eng A-Struct* **360** 126-131. DOI: [https://doi.org/10.1016/S0921-5093\(03\)00376-9](https://doi.org/10.1016/S0921-5093(03)00376-9)
- [12] Wayman C M and Duerig T W, 1990 An Introduction to Martensite and Shape Memory, Engineering aspects of Shape Memory Alloys, Ed. Duerig T W, Melton K N, Stockel D and Wayman C M (Butterworth-Heinemann Ltd., London, UK) p.11.
- [13] He Z, Gall K R and Brinson L C, 2006 Use of Electrical Resistance Testing to Redefine the Transformation Kinetics and Phase Diagram for Shape-Memory Alloys, *Metall Mater Trans A* **37** 579-587. DOI: <https://doi.org/10.1007/s11661-006-0030-1>